Astron. Astrophys. 321, 151–158 (1997)

ASTRONOMY AND ASTROPHYSICS

Magnetic field generation in close binary systems

David Moss[1] **and Ilkka Tuominen**[2]

[1] Mathematics Department, The University, Manchester M13 9PL, UK
[2] Department of Geosciences and Astronomy, P.O. Box 333, University of Oulu, FIN-90571 Oulu, Finland

Received 24 January 1996 / Accepted 6 September 1996

Abstract. A simple mean field dynamo model is developed and applied to two 'dynamo-active' components of a close or contact binary system. Tidal interaction is assumed to reduce differential rotation to such a degree that the dynamo action is of 'α^2' type. A variety of nonaxisymmetric magnetic fields are produced, steady and unsteady, of both odd, even and mixed parity with respect to the equatorial plane. The relevance of the solutions to evidence for large-scale fields in close and contact binary systems is discussed.

Key words: MHD – binaries: close – stars: late type – stars: magnetic fields

1. Introduction

Indications of magnetic activity have been detected in a variety of late type stars in close binary systems, including (detached) RS CVn systems and contact systems of W UMa class. Although the solar field is predominantly axisymmetric, there is evidence even there for some nonaxisymmetric large-scale features (solar 'sector structure', and see Jetsu et al. 1996, preprint), and there is much stronger evidence for nonaxisymmetry in some other single stars and RS CVn-type binaries, both from the analysis of long time series of photometric data (eg Jetsu et al. 1993, 1994; Jetsu 1996), and from photometric modelling (eg Bradstreet 1985; Zeilik et al. 1989, 1990a, 1990b; Henry et al. 1995). Snapshots of this kind of spot structure have been derived by surface imaging techniques (eg Piskunov, Tuominen and Vilhu 1990; Piskunov, Ryabchikova and Tuominen, preprint). There is also the possibility of using eclipses to image binaries (Vincent, Piskunov and Tuominen, 1993; Vincent et al., in preparation). The conventional view is that magnetic activity in late-type stars is the result of dynamo action in their deep convective envelopes, and this has been studied in single stars by a large number of authors. However, for some time large-scale nonaxisymmetric structures of the kinds indicated by the above-quoted and other papers seemed difficult to explain in the context of mean field dynamo theory. More recently a number of mechanisms have been identified that can result in the excitation of stable nonaxisymmetric fields, provided that the differential rotation is not too strong (Rädler et al 1990; Moss, Brandenburg and Tuominen 1991; Moss & Brandenburg 1993; Rüdiger & Elstner 1994; Moss et al 1995). If both stars of a close binary are dynamo-active, then it is easier to envisage the excitation of large-scale nonaxisymmetric fields – the geometry of the system is intrinsically nonaxisymmetric and tidal interactions can be expected to reduce severely the differential rotation and, indeed, to lock the spin and orbital frequencies.

Thus, in this paper we study dynamo action in two corotating spheres that may be separate, touch or partially overlap. Two touching or overlapping spheres provide only a poor geometric approximation to the Roche geometry of contact or over-contact binary systems, but we feel that the essentially nonaxisymmetric geometry is represented to an adequate first approximation. We recognize that dynamo action can be expected to be limited to a thick outer envelope, but for reasons of computational convenience and economy we assume the dynamo-active regions to occupy the entire volumes of the spheres. The two dynamo-active spheres are embedded in a 'computational sphere', at the surface of which vacuum boundary conditions are applied. Within this computational sphere, the diffusion coefficient is assumed everywhere uniform, but the α-coefficient is only nonzero within the dynamo-active region(s), thus implying that α is a function of azimuthal coordinate measured about an axis parallel to the rotation axis (cf Moss et al 1991). We ignore the effects of any large-scale circulation: this approximation might be especially inappropriate for common envelope systems. Overall, the computational philosophy has some similarity to that of the 'embedded disc' galaxy codes (Stepinsky & Levy 1988; Elstner, Meinel and Rüdiger 1990; Moss & Tuominen 1990). The code used is essentially that described in Moss et al (1991).

2. The model

We consider two dynamo-active spheres, radii r_1, r_2 contained within a spherical computational volume of normalized radius unity. For many of the calculations we placed the origin of spherical polar coordinates (r, θ, ϕ) at the centre of the computational volume. whose surface was thus tangent to both of the dynamo-

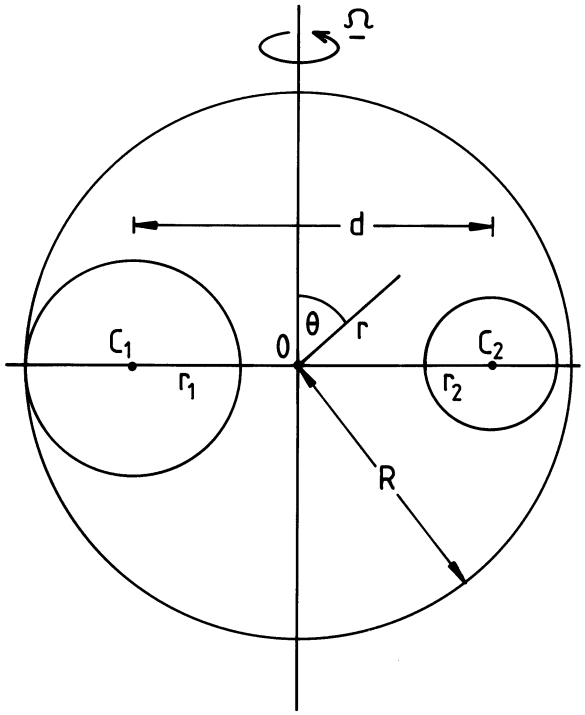

Fig. 1. Schematic cross-section through line of centres and rotation axis. The outer circle represents the intersection of the cross-section with the surface of the computational volume. When O is at the centre of the volume, this circle is tangent to both the circles radius r_1 andr_2.

active spheres. The separation of the centres, d, then satisfies $r_1 + r_2 + d = 2$, and the axis of the coordinate system is parallel to the orbital angular velocity vector. Fig. 1 shows a cross-section through a plane containing the rotation axis, and also a section through the equatorial plane. More realistically, the origin should be at the centre of mass of the system, which needs some assumption such as

$$R_* \propto M_*^p, \tag{1}$$

where R_*, M_* are the radius and mass of a component, in order to determine fully the geometry. (For equal radii, $r_1 = r_2$, the models are identical.) A relation such as this imposes a geometrical constraint on possible configurations; thus calculations with $r_1 \neq r_2$, and origin not at the centre of mass, should be regarded as perhaps less realistic. However, trials show that results do not differ generically between these slightly different configurations. In relation (1), we take $p = 0.7$ for non-contact, and $p = 0.5$ for contact, configurations, corresponding approximately to the standard relations for detached and contact lower main sequence systems. An alternative assumption to that described below is that $\alpha \propto z = r\cos\theta$, which removes the distinction between use of the two different origins of coordinates as discussed above. Test calculations with this assumption give similar behaviour to those with $\alpha \propto \cos\theta$, for rather larger values of α.

A conventional α-effect is taken in the form $\alpha = \alpha^* f(\mathbf{B})\cos\theta$ inside the dynamo-active regions, where α^* is a constant, and $\alpha = 0$ outside. Thus, within the computational sphere, we can write $\alpha = \alpha_0(r,\theta,\phi)f(\mathbf{B})$, where

$$\alpha_0(r,\theta,\phi) = \sum_{m=0} \alpha_m(r,\theta)\cos m\phi. \tag{2}$$

The coefficients α_m can readily be determined analytically when $r_1 = r_2$, but in general were evaluated numerically. A standard α-quenching nonlinearity,

$$f(\mathbf{B}) = \frac{1}{1+\mathbf{B}^2(r,\theta,\phi,t)}, \tag{3}$$

was used to limit the solutions at finite amplitude. The non-dimensional dynamo parameter is $C_\alpha = \alpha^* R/\eta$, where R is the radius of the computational sphere (Fig 1), and η is the diffusivity, assumed constant throughout the computational sphere. Rotation is assumed uniform, and so there is no corresponding dynamo number to quantify differential rotation – this is strictly an 'α^2 dynamo'. On the surface of the computational volume, vacuum boundary conditions are applied. In general, α will contain contributions from all azimuthal Fourier modes, see Eq. (2). Correspondingly, the nonlinearity (3) means that the dynamo field will in general be of the form

$$\mathbf{B}(r,\theta,\phi) = \sum_{m=0}^{\infty} \mathbf{B}_m(r,\theta)\exp(im\phi), \tag{4}$$

ie all Fourier modes will be present in **B** also.

Thus the system has three important parameters: r_1, r_2, C_α. Comparison between solutions with different values of r_1, r_2 is complicated by the changing value of C_α for which the dynamo is first excited, $C_{\alpha c}$ say. This can be thought of as being, in part at least, due to the relative volume where $\alpha \neq 0$ decreasing as the separation increases (ie as r_1 and r_2 decrease). We did not attempt to derive systematically $C_{\alpha c}$ values.

For the case where the binary radii are equal, certain symmetries in the solution can be predicted. In this case α contains only terms proportional to $\cos 2m\phi$, $m = 0, 1, 2, ...$ Thus dy-

Table 1. Summary of results for equal stellar radii, $C_\alpha = 100$. A - in the 5th column indicates that $m = 1$ fields were not present. The column headed 'type' distinguishes steady and oscillating solutions. An entry of two bracketed values indicates the range of variation of an oscillatory quantity. $\pm$ after an entry indicates small oscillations near the tabulated value.

r_b	E_{TOT}	O/E/W	P	P_1	M	type
0.7	7.5	E	-1	-	0.07	steady
0.6	4.4	E	-1	-	0.13	steady
0.55	3.0	E	-1	-	0.23	steady
0.5	1.65$\pm$	O+E	(-0.80,-0.78)	1	(0.48,0.51)	osc
0.475	1.2	O	-1	-1	1.0	steady
0.45	0.7	O	-1	-1	1.0	steady
0.425	0.5	O	-1	-1	1.0	steady
0.410	0.4$\pm$	O	1	1	1.0	osc
0.40	0.3$\pm$	O	1	1	1.0	osc

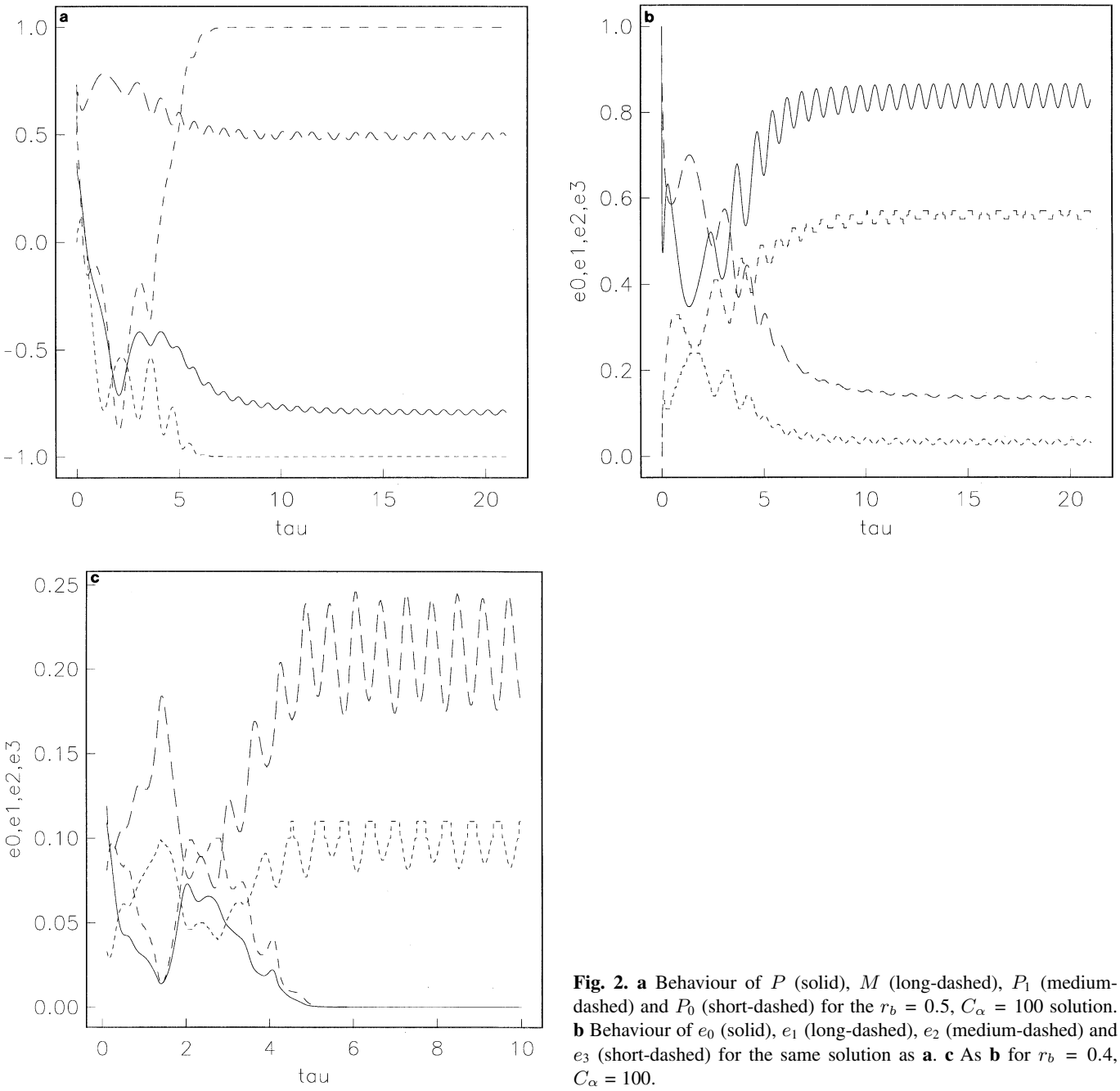

Fig. 2. **a** Behaviour of P (solid), M (long-dashed), P_1 (medium-dashed) and P_0 (short-dashed) for the r_b = 0.5, C_α = 100 solution. **b** Behaviour of e_0 (solid), e_1 (long-dashed), e_2 (medium-dashed) and e_3 (short-dashed) for the same solution as **a**. **c** As **b** for r_b = 0.4, C_α = 100.

Table 2. Summary of results for equal stellar radii, other values of C_α.

C_α	r_b	E_{TOT}	O/E/W	P	P_1	M	type
300	0.3	(0.22-0.25)	O	(-.65,-.13)	(-.70,-.12)	1	osc
40	0.7	2.24	E	-1	-	0.04	steady
40	0.5	0.33	E	-0.99	-	0.38	steady
40	0.4	0.003±	O	1	1	1	osc

namo solutions fall into two azimuthal symmetry families, with the field written symbolically as

$$\mathbf{B}_{\text{even}} = \sum_{m=0} \mathbf{B}_{2m} \exp(i2m\phi), \tag{5}$$

and

$$\mathbf{B}_{\text{odd}} = \sum_{m=0} \mathbf{B}_{2m+1} \exp(i(2m+1)\phi). \tag{6}$$

This follows directly from the form of nonlinearity (3). For given parameters either or both or neither of these families may be excited. We can refer to family (5) as of type E, and to (6) as of type O. If both are simultaneously excited (O+E), then there will be no direct modal interactions. However the nonlinearity (3), being local, will then give an indirect interaction between odd and even field components, the odd symmetry field being able to quench the dynamo growth of the even in a spatially nonuniform manner, and vice versa.

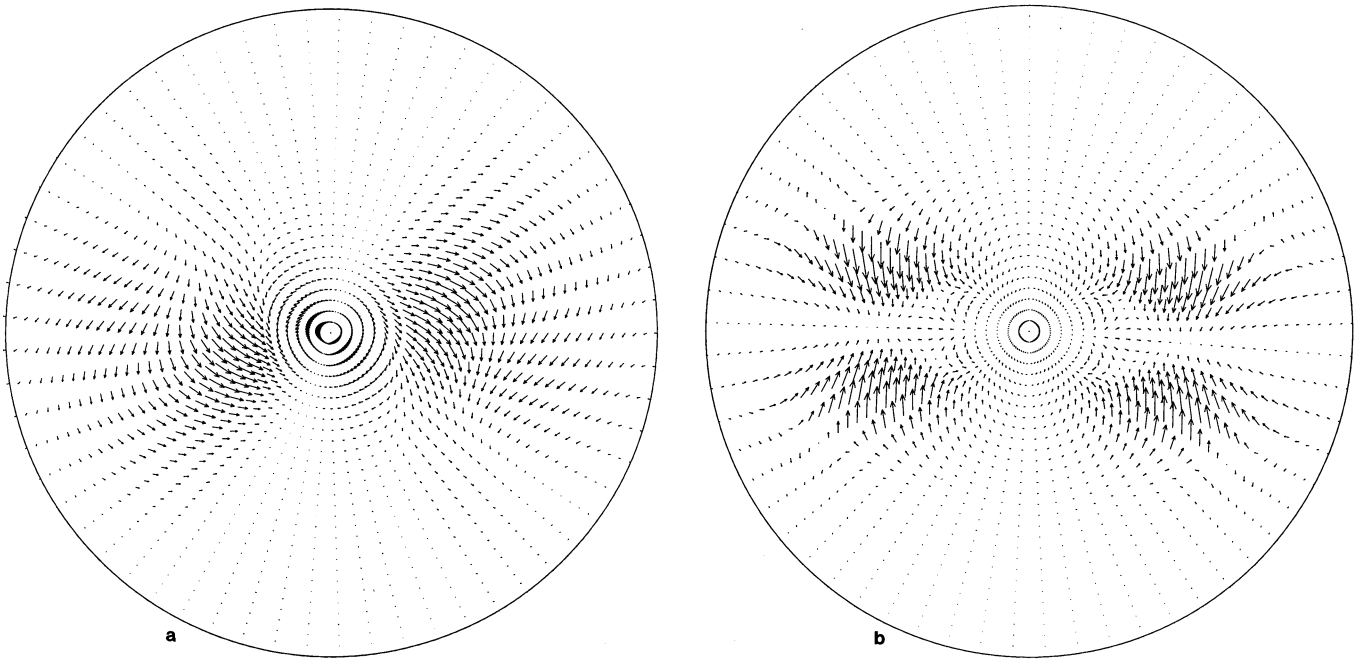

Fig. 3a and b. r_b = 0.4, C_α = 100. **a** Field vectors in the equatorial plane, projected on to that plane. The line of centres passes horizontally through the centre of the figure. ϕ = 0 is to the right and ϕ increases anticlockwise. The enclosing circle is the projection of the computational volume. **b** Field vectors in the plane ϕ = 0, projected on to that plane. The rotation axis passes vertically through the centre of the figure.

Table 3. Summary of results for detached configurations with unequal stellar radii. A † indicates computations with the origin of coordinates at the centre of mass.

C_α	d	r_1	r_2	E_{TOT}	O/E/W	P	P_1	M	type
100	1.2	0.3	0.5	(.77,.79)	W	1	1	(0.75,0.90)	osc
100	1.2	0.35	0.45	0.45	W	1	1	0.93	steady
200	1.2	0.35	0.45	1.29	W	1	1	0.95	steady
100	1.3	0.50	0.20	0.79	W	-1	-1	0.85	steady
100	1.05	0.487	0.300	(0.94,0.96)	W	1	1	(0.41,0.92)	osc†
200	1.05	0.487	0.300	2.26±	W	1	1	(0.40,0.92)	osc †
40	0.95	0.617	0.200	0.88	W	-1	-1	0.17	steady†
100	0.95	0.617	0.200	3.08	W	-1	-1	0.18	steady†
100	1.10	0.452	0.353	0.59	W	1	1	0.85	steady†
100	1.092	0.453	0.353	0.59	W	0.87	0.82	0.82	steady†

In the more general case of unequal radii, where all Fourier components of α are non-zero, the magnetic field will also contain all Fourier components (type W, say). However, if the radii are comparable, but not equal, the even-m contributions to α will still dominate. If the nearby solution for strictly equal radii is of odd or even type with respect to m, then it can be expected that the solution for unequal radii will be dominated by this solution, with only a relatively small component of the opposite symmetry type present. If E_{TOT}, $E(0)$ are respectively the total magnetic energy and that contained in the axisymmetric part of the field, then $M = 1 - E(0)/E_{TOT}$, $0 \leq M \leq 1$, is a measure of the global azimuthal symmetry. The energies, e_m, in the mth mode can also be calculated.

The other useful global symmetry parameter is the parity. If (A), (S), denote fields with radial components that are respectively odd, even with respect to the plane $\theta = \pi/2$, and $E(A)$, $E(S)$ are the corresponding parts of the total magnetic energy, then $P = (E(S) - E(A))/(E(S) + E(A))$, with $-1 \leq P \leq 1$ (cf Moss et al 1991). Parity parameters P_m can also be defined for the individual azimuthal Fourier modes.

In the limit $r_1 = r_2 \rightarrow 1$, the spheres are almost superimposed, and the overall dynamo-active volume approaches a sphere. The solutions should then approach the known solution for a sphere. We computed the marginal value of C_α when $r_1 = r_2 = 0.98$, $d = 0.04$, to be approximately 7.75, with $P_0 = -1$. This is consistent with the standard marginal value of $C_{\alpha c} = 7.64$ for the first bifurcation from the trivial solution to a dipolar axisymmetric field for the spherical α^2 dynamo.

We note that the problem could have been tackled by taking the line of centres as the axis $\theta = 0$ of the polar coordinate

system, with $\alpha \propto \sin\theta\cos\phi$ within the dynamo-active regions. A trial calculation with $r_1 = r_2$ was found to agree reasonably well with results obtained with the geometric configuration used above, but this approach seemed less flexible, and so was not pursued.

The code used is an adaption of that described in Moss et al (1991). An explicit $NI \times NJ$ grid in r and θ is used, together with a modal expansion in ϕ, including modes $0 \leq m \leq N_m$. Experience suggested that NI = 31, NJ = 61, N_m = 5 was adequate for the parameters used. The dimensionless time, τ, is measured in units of R^2/η.

We note that, despite some perhaps superficial similarities, this work does not describe a dynamo of Herzenberg type (Herzenberg, 1958). In our case the spin axes are assumed to be strictly aligned, and the components do not spin relative to one another. Some related issues connected with the Herzenberg dynamo are discussed in Brandenburg, Moss and Soward, in preparation.

3. Results and discussion

We begin by considering the case of equal radii, $r_1 = r_2 = r_b$, say, and vary the separation of the centres. We take a fixed value, C_α = 100, at which a dynamo is excited over a wide range of radii, r_b. Calculations are usually started from an arbitrary configuration containing a mixture of m = 0 and m = 1 components, with $P \neq \pm 1$. Results are outlined in Table 1. For r_b = 0.3, the dynamo is not excited at C_α = 100. This sequence of computations exhibits several interesting features. For $0.7 \geq r_b \geq 0.55$, the solutions are steady, of type E, and have $P = -1$. M increases as r_b decreases and the relative separation of the centres increases. For $0.475 \geq r_b \geq 0.425$, the solutions are steady, of type O, and $P = -1$. The behaviour for larger r_b (ie smaller separation of centres) is consistent with the limit $d \to 0$, as discussed in Sect. 2. For r_b = 0.5, both O and E type solutions coexist. Here P_1 = 1, so the overall solution is of mixed parity, $P \neq \pm 1$, and it is oscillatory. For values of r_b a little smaller than 0.5, the O-type solutions disappear, and solutions are again steady. Between r_b = 0.425 and 0.410 there is a further bifurcation, and the stable solution becomes oscillatory, with constant parity P = 1. In Fig. 2 we show some details of the temporal behaviour of the r_b = 0.5 and r_b = 0.4 solutions, and Fig. 3a,b gives field vectors projected on to equatorial and azimuthal planes when r_b = 0.4. In Fig. 4a,b for the r_b = 0.4 calculations we give contours of radial and absolute field at the surface of the computational sphere, and in Fig. 4c,d the corresponding quantities at the surface of one of the dynamo-active component spheres.

In Table 2 we present several other calculations for equal radii, but with different C_α values. No significant changes in behaviour are apparent from those with C_α = 100, except that when C_α = 40, the r_b = 0.5 solution is steady and that with r_b = 0.40 is only marginally excited.

Table 2 gives results from computations for detached configurations of unequal radii. As anticipated, the solutions are now of type W, and so, necessarily, $M \neq 1$. Usually the solutions are of 'pure' parity, $P = \pm 1$, but we did discover some stable 'mixed parity' solutions. Solutions can be either oscillatory or steady. In some cases, very long-lived transient behaviour is observed, over as long as 50 or more global diffusion times. In the cases with $(r_1, r_2, d) = (0.617, 0.200, 0.95)$ in Table 2, the fields appear to be settling to a P = +1 configuration when, after 10–15 diffusion times a relatively sudden change to $P = -1$ occurred, accompanied by a decrease in M from near unity to the tabulated values. We show details of the evolution of parity and M with time for this case in Fig. 5a, and of the energies for the case (r_1, r_2, d) = (0.4874, 0.30, 1.05), C_α = 200 in Fig. 5b. As anticipated in Sect. 2, solutions listed in Table 2 with (d_1, r_1, r_2) values close to those of the O-type solutions in Table 1 do have the majority of the energy in the odd m field modes. In Fig. 6a,b we show field contours over the surface of the computational sphere, and the surface of the primary component, for the solution shown in Fig. 5b. The last entry of Table 2 is noteworthy. Although the parameters are only slightly different from those of the immediately preceding entry, its behaviour is quite different in that the fields are not then of pure parity, P = 1.

In Table 3 there are results for contact configurations of unequal radii. These solutions are all of type W and are steady with $P = -1$..

Table 4. Summary of results for contact configurations with unequal stellar radii. A † indicates computations with the origin of coordinates at the centre of mass.

C_α	d	r_1	r_2	E_{TOT}	O/E/W	P	P_1	M	type
25	1.0	0.7	0.3	0.57	W	-1	-1	0.41	steady
40	1.0	0.7	0.3	1.32	W	-1	-1	0.42	steady
100	1.0	0.7	0.3	4.51	W	-1	-1	0.48	steady
200	1.0	0.7	0.3	10.0	W	-1	-1	0.48	steady
100	1.0	0.5	0.7	5.35	W	-1	-1	0.20	steady
100	0.89	0.576	0.315	2.25	W	-1	-1	0.20	steady†
100	0.75	0.71	0.50	4.96	W	-1	-1	0.16	steady†

4. Concluding remarks

We recognize that the model investigated in this paper is very idealized, and so the solutions discussed can only be considered to be illustrative. Nevertheless we believe that we have captured something of the essence of the physical situation, and that the solutions presented do have some relevance to the richness and wide variety of behaviour that can be expected in a close binary comprising two late-type stars. The solutions are naturally nonaxisymmetric. However this is more than just the obvious asymmetry obtained, eg, by viewing two individual, almost axisymmetric, stars from a distance. The 'natural' parity of a spherical dynamo, or of two such fields viewed together, is odd ($P = -1$). We see from Tables 1 - 3 that many of the solutions are even with respect to the orbital plane (P = +1). We emphasize that we have taken the simplest form of nonlinear dynamo, without inclusion of any of the effects that have previously been shown to favour the growth of nonaxisymmetric fields, such as nonuniform distribution of dynamo source terms (Rädler et al

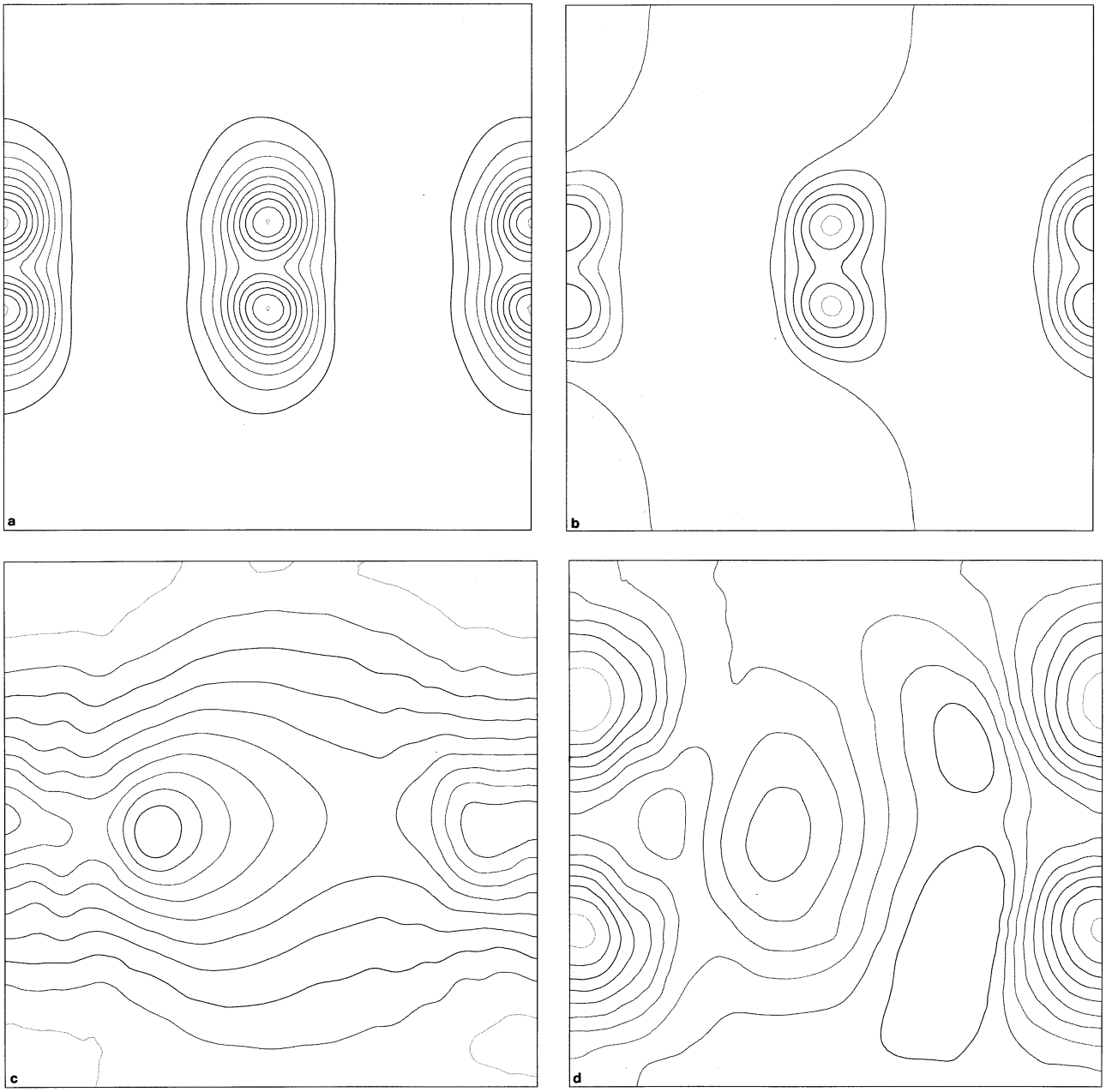

Fig. 4a–d. r_b = 0.4, C_α = 100. **a** Contours of radial field strength on the surface of the computational sphere. **b** Contours of absolute field strength on the surface of the computational sphere. ϕ runs horizontally from $-\pi$ to π, θ vertically from 0 (top) to π (bottom). **c** Contours of radial field strength on the surface of the primary component. **d** Contours of absolute field strength on the surface of the primary component. In **c** and **d**, if Θ, Φ are spherical coordinates measured with respect to the spin axis of the primary, then Θ runs from $\Theta = 0$ (top) to $\Theta = \pi$, and Φ from 0 to 2π horizontally, where $\Phi = 0$ corresponds to the direction of the centre of the secondary

1990; Moss et al 1991), anisotropy of α (Rüdiger & Elstner 1994) or dynamically driven large-scale motions in meridional planes, perhaps with a latitudinally dependent angular velocity (Moss et al 1995). The sensitivity of the solutions to the imposed parameters in certain ranges is hinted at by the last entry of Table 2, where a small change in the parameters alters quite radically the solution. There are other indications of the presence of uninvestigated bifurcations as the physical parameters are altered: the computations are sufficiently time-consuming, and the model too preliminary, for it to be yet worthwhile to explore this issue systematically

We can deduce that close late-type binaries can be expected to exhibit large-scale nonaxisymmetric fields. These may be of even parity, especially if the components are detached (Tables 1 and 2), which is not the parity of the stable solutions for the individual stars. The visible fields then have maxima at the longitudes corresponding to the intersection of the line of centres with the stellar surfaces. We believe that these results may

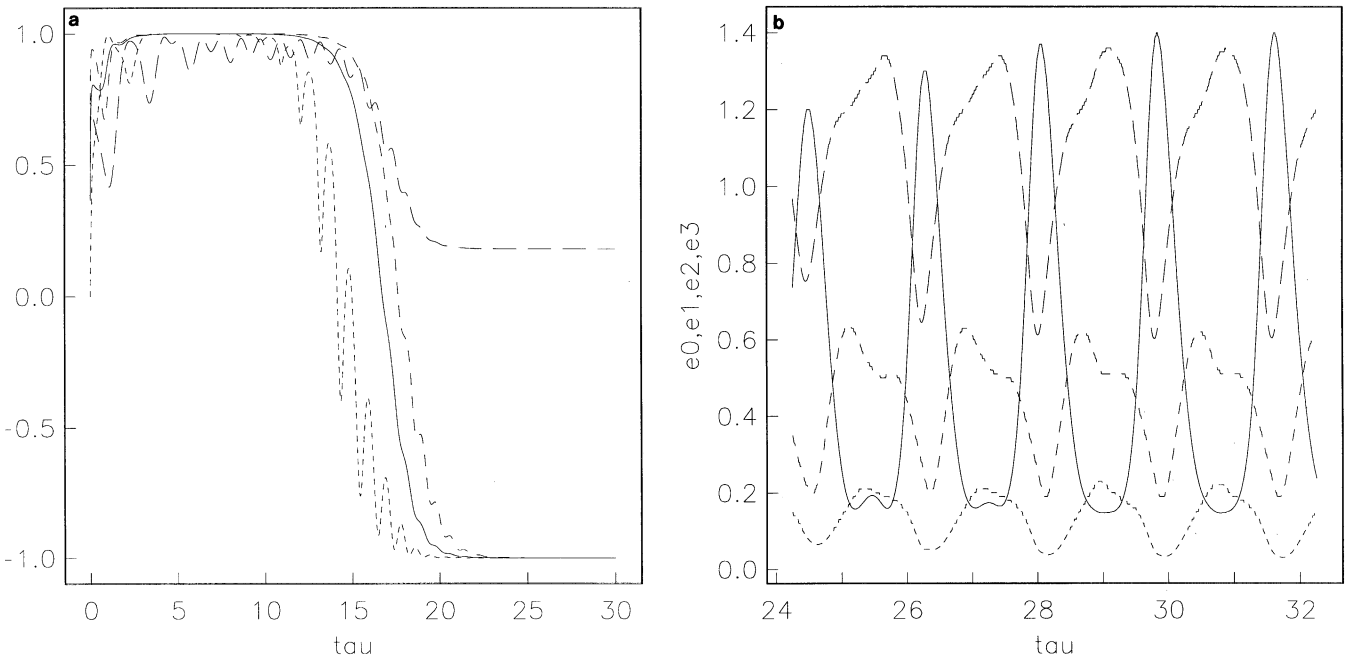

Fig. 5. a Evolution of P, M, P_1, P_0 when C_α = 100, (r_1, r_2, d) = (0.617, 0.20, 0.95), as Fig. 3a). Temporal behaviour of modal energies e_0, e_1, e_2, e_3, for C_α = 200, (r_1, r_2, d) = (0.4874, 0.30, 1.05) calculation, as Fig. 3b)

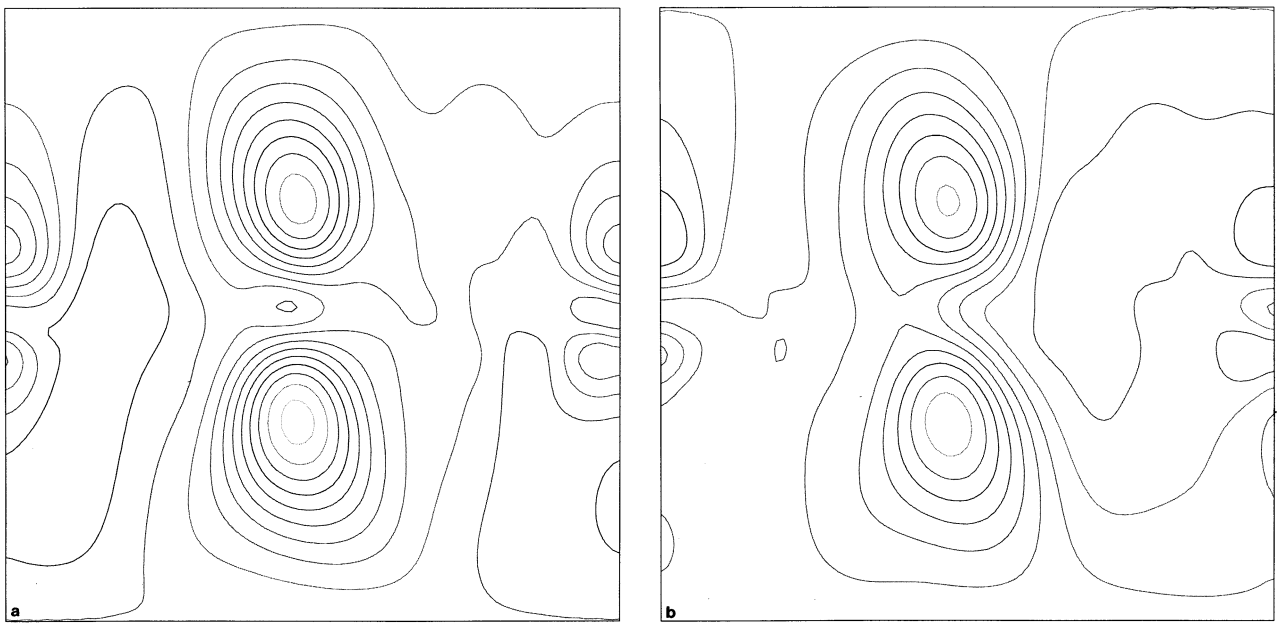

Fig. 6a–d. C_α = 200, (r_1, r_2, d) = (0.4874, 0, 30, 1.05). **a** Contours of radial field strength over surface of computational sphere. **b** Contours of absolute field strength on the surface of the computational sphere. **c** Contours of radial field strength on the surface of the primary component. **d** Contours of absolute field strength on the surface of the primary component. Orientation is as described for Fig. 4

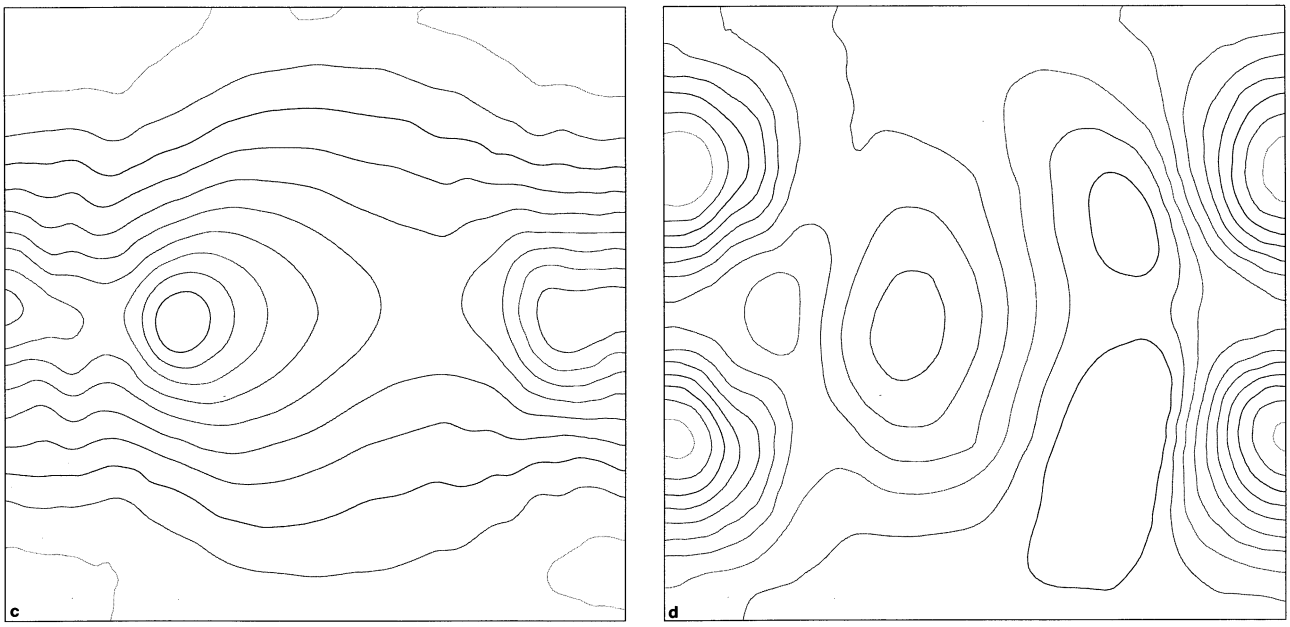

Fig. 6a–d. continued

have relevance to the preferred longitudes of active regions on the surfaces of RS CVn systems, as referenced in the Introduction.

Acknowledgements. The authors thank John Brooke for his comments. This work was supported by EC HCM grant 'Late-type stars: activity, magnetism, turbulence', ERBCHRXCT940483.

References

Bradstreet, D.H., 1985, Astrophys. J. Suppl. Ser. 58, 413
Elstner, D., Meinel, R., Rüdiger, G., 1990, Geophys. Astrophys. Fluid Dyn. 50, 85
Herzenberg, A., 1958, Phil. Trans. R. Soc. A., 250, 543
Henry, G.W., Eaton, J.E., Hamer, J., Hall, D.S., 1995, Astrophys. J. Suppl. Ser., 97, 513
Jetsu, L., 1996, Astron. Astrophys., in press
Jetsu, L., Pelt, J., Tuominen, I., 1993, Astron. Astrophys. 278, 449
Jetsu, L., Tuominen, I., Grankin, K.I., Mel'nikov, S. Yu., Shevchenko, V.S., 1994, Astron. Astrophys. 282, L9
Moss, D., Tuominen, I., 1990, Geophys. Astrophys. Fluid Dyn. 50, 113
Moss, D., Brandenburg, A., Tuominen, I., 1991, Astron. Astrophys. 247, 576
Moss, D., Brandenburg, A., 1993, in 'Solar and Planetary Dynamos', eds M.R.E. Proctor, P.C. Matthews, A.M. Rucklidge (C.U.P., Cambridge), p. 219
Moss, D., Barker, D.M., Brandenburg, A., Tuominen, I., 1995, Astron. Astrophys. 294, 155
Piskunov, N.E., Tuominen, I., Vilhu, O., 1990, Astron. Astrophys. 294, 155
Rädler, K.-H., Wiedemann, E., Brandenburg, A., Meinel, R., Tuominen, I., 1990, Astron. Astrophys. 239, 413
Rüdiger, G., Elstner, D., 1994, Astron. Astrophys. 281, 46
Stepinsky, T.F., Levy, E.H., 1988, Astrophys. J., 331, 416
Vincent, A., Piskunov, N.E., Tuominen, I., 1993, Astron. Astrophys. 278, 523
Zeilik, M., Cox, D.A., de Blasi, C., Rhodes, M., 1989, Astrophys. J.,345, 991
Zeilik, M., Ledlow, M., Rhodes, M., Arévalo, M.J., Budding, E., 1990a, Astrophys. J., 354, 352
Zeilik, M., Cox, D.A., Ledlow, M., Rhodes, M., Heckert, P.A., Budding, E., 1990b, Astrophys. J., 363, 647

This article was processed by the author using Springer-Verlag LaTeX A&A style file *L-AA* version 3.